In-Plane Co_9S_8@MoS_2 Heterostructure for Hydrogen Evolution Reaction in Alkaline Media

Lechen Diao [a], Biao Zhang[a], Qiaozhi Sun[a], Ning Wang[a], Qiaozhi Sun[a], Naiqin Zhao[a,b,c], Chunsheng Shi[a], Enzuo Liu[a,b,], and Chunnian He [a,b,c,*]

[a] School of Materials Science and Engineering and Tianjin Key Laboratory of Composites and Functional Materials, Tianjin University, Tianjin, 300072, P. R. China

[b] Collaborative Innovation Center of Chemical Science and Engineering, Tianjin 300072, China

[c] Key Laboratory of Advanced Ceramics and Machining Technology, Ministry of Education, Tianjin University, Tianjin, 300072, China.

* Corresponding Authors.

cnhe08@tju.edu.cn (C. He)).

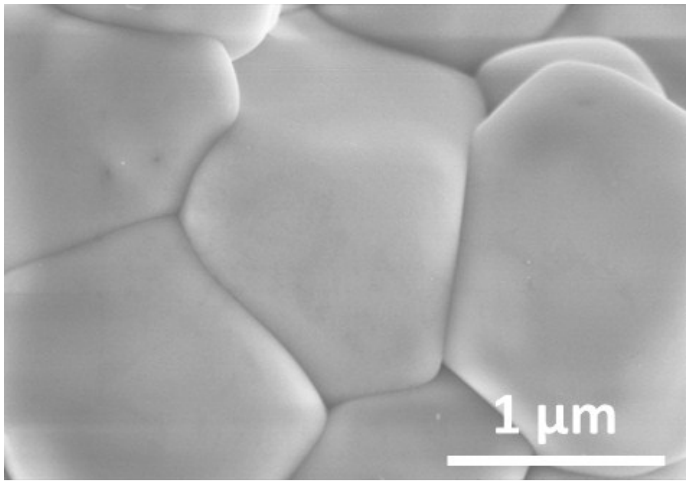

Figure S1. $C_6H_8O_7$-$Co(NO_3)_2$-NH_2CSNH_2-$(NH_4)_6Mo_7O_{24}$ complex wrap on the surface of the NaCl crystals.

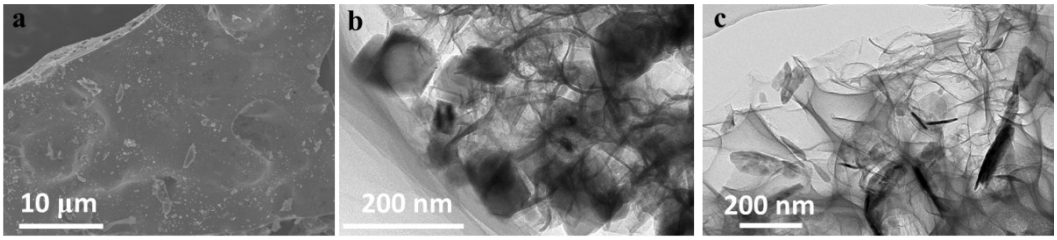

Figure S2. TEM of (a) Co_9S_8-MoS_2@C, (b) Co_9S_8@3DC and (c) MoS_2@3DC.

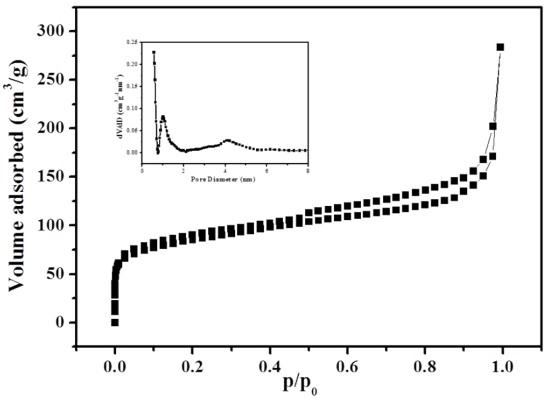

Figure S3. BET surface area of Co_9S_8-MoS_2@3DC. Insert is the BJH pore size distribution.

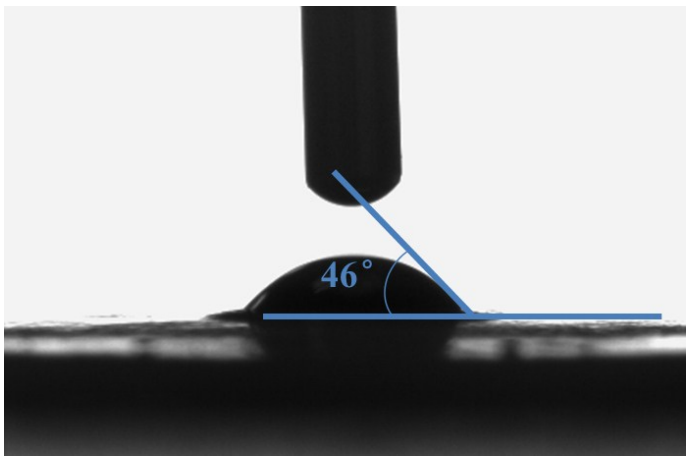

Figure S4. Static contact angle of Co_9S_8-MoS_2@3DC.

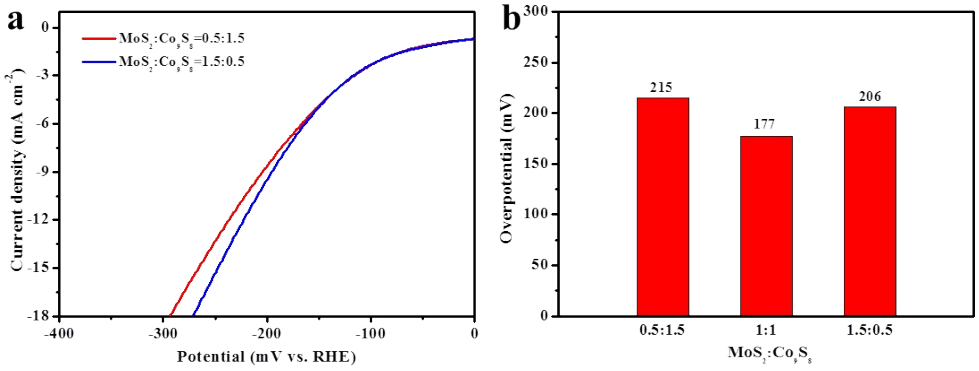

Figure S5. HER performance of MoS_2-Co_9S_8@3DG with different ratio of MoS_2 to Co_9S_8 (0.5:1.5, 1:1, 1.5:0.5)

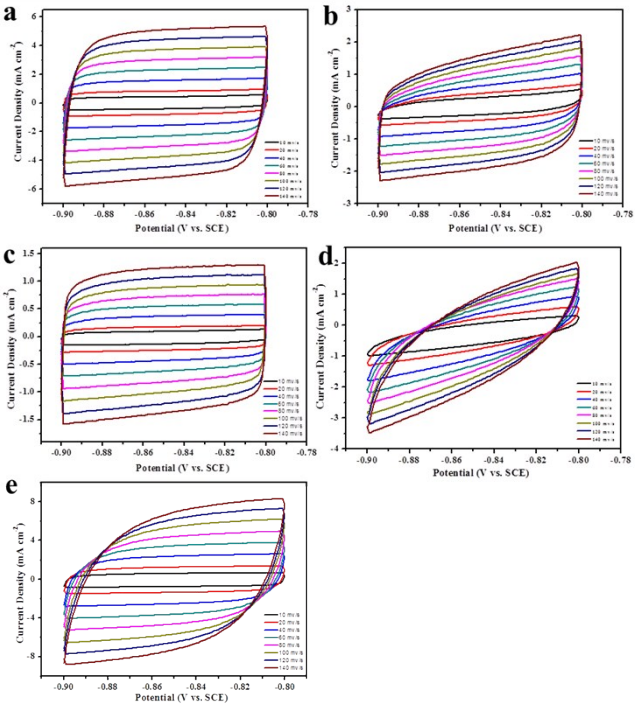

Figure S6. Cyclic voltammograms in the region of -0.9 — –0.8 V vs. SCE. (a) Co_9S_8-MoS_2@3DC, (b) Co_9S_8@3DC, (c) MoS_2@3DC, (d) Co_9S_8-MoS_2@3DC, and (e) N S doped C.

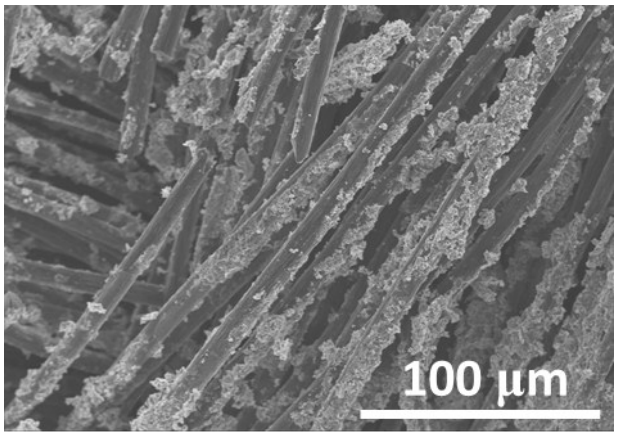

Figure S7. SEM image of catalysts on the carbon clothes after i-t test at 50 mA cm^{-2}.

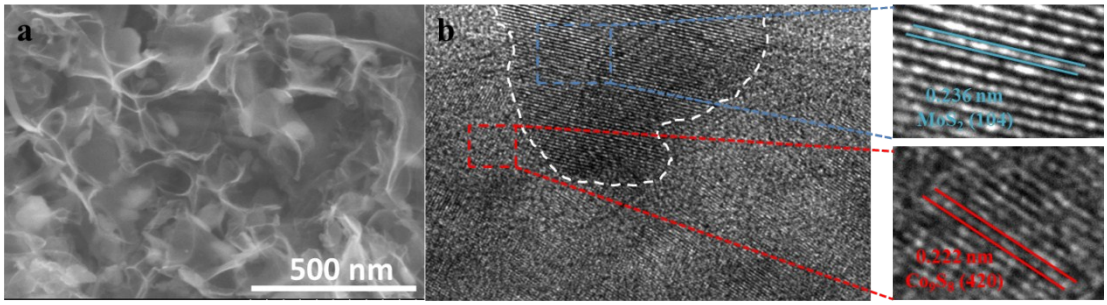

Figure S8. (a) SEM and (b) HRTEM images of catalysts after i-t test.

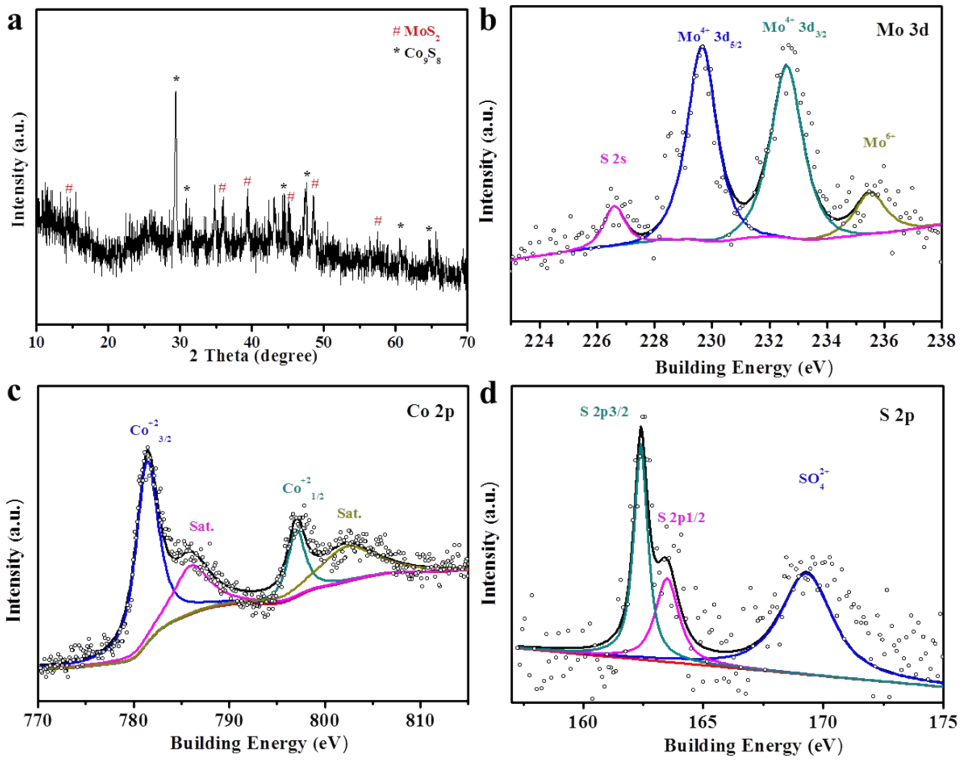

Figure S9. (a) XRD and (b-c) XPS images of catalysts after i-t test.

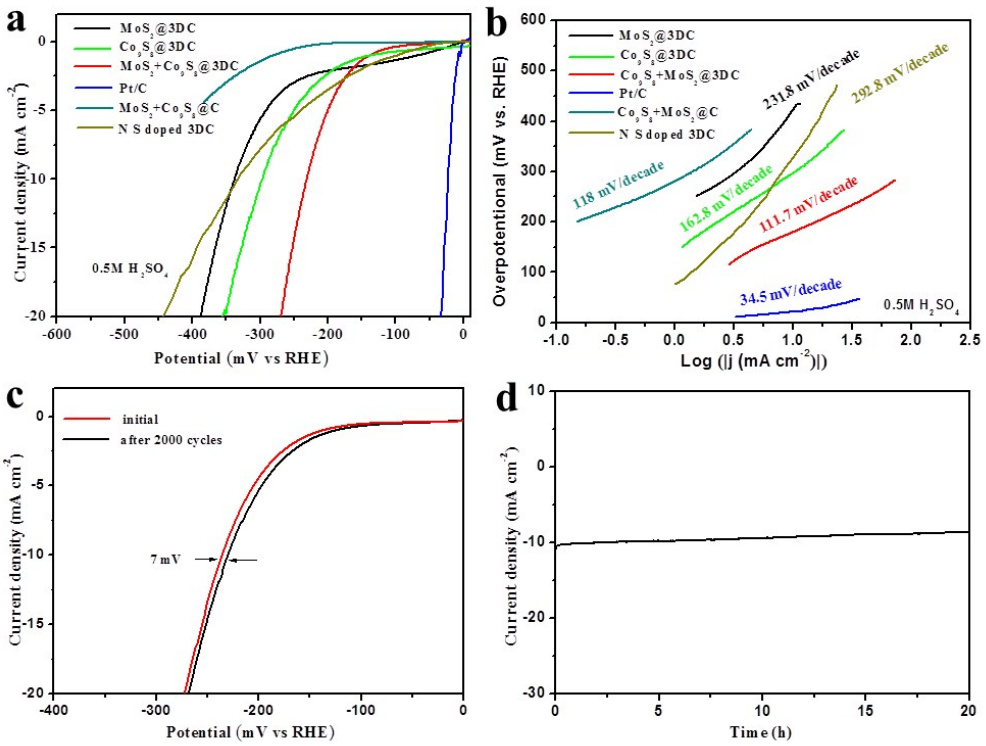

Figure S10. (a) polarization curves, (b)Tafel slope, of Co_9S_8-MoS_2@3DC, Co_9S_8@3DC, MoS_2@3DC, and Co_9S_8-MoS_2@3DC in 0.5 M H_2SO_4. (c) Cathodic linear sweep voltammograms of Co_9S_8-MoS_2@3DC for the first and 2000th CV cycles in 0.5 M H_2SO_4. (d) Long-term chronoamperometric test performed at overpotential of 230 mV in 0.5 M H_2SO_4.

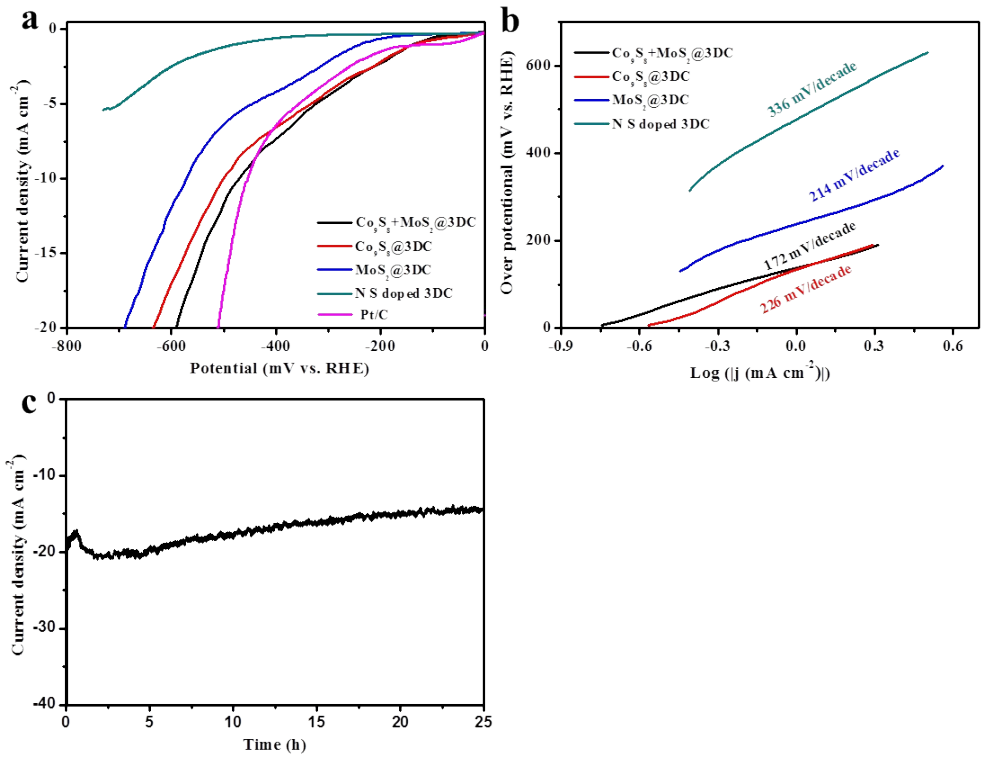

Figure. S11. (a) polarization curves and (b)Tafel slope of Co_9S_8-MoS_2@3DC, Co_9S_8@3DC, MoS_2@3DC, Co_9S_8-MoS_2@3DC, and N, S doped C in 1 M PBS. (c) Long-term chronoamperometric test performed at overpotential of 470 mV in 1 M PBS.

Table S1. Performance comparison of the HER activity in alkaline electrolyte

catalyst	Current density j=10mA cm^{-2}	ŋ at corresponding j (mV)	Tafel slope ($mV•dec^{-1}$)	Reference
Co-WSe_2/MWNTs	10	241		J. Mater. Chem. A, 2018,6, 4793-4800
MoS_2/graphene/Ni foam	10	> 600	98	Adv. Func. Mater., 2014, 24(39): 6123-6129.
Co_3S_4@MoS_2	10	310	59	Chem. Mater. 2017, 29, 5566−5573
Co_9S_8@MoS_2/CNFs	10	361	61	Adv. Mater. 2015, 27, 4752-4759
MoS_2/Ni_3S_2	10	218	88	Angew. Chem. Int. Ed. 2016, 55, 6702-6707.
Carbon Paper/Carbon Tubes/CobaltSulfide	10	306	72	ACS Nano 2016, 10, 2342-2348
CoMoSx	10	190	124	ACS Appl. Mater. Interfaces2019112421634-21644

Co_9S_8+Ni_3S_2/Ni	10	278	-	Electrochimica Acta, 2019, 299: 152-162.
Co_3S_4/MoS_2/Ni_2P	10	178	98	J. Mater. Chem. A 2017, 5, 25410-25419
$CoSe_2$–$MoSe_2$/rGO-C	10	215	83.2	J. Mater. Chem. A 2018, 6, 12701-12707.
Co_9S_8@MoS_2/CNFs	10	190	110	Adv. Mater. 2015, 27, 4752–4759